Storage ring study of the mutual neutralisation of N^+ with O^-

Mathias Poline,* Stefan Rosén, MingChao Ji, Ansgar Simonsson, Peter Reinhed, Mats Larsson, Henning T. Schmidt, and Richard D. Thomas†
Department of Physics, Stockholm University, Stockholm SE-10691, Sweden

Arnaud Dochain and Xavier Urbain
Institute of Condensed Matter and Nanosciences, Université Catholique de Louvain, Louvain-la-Neuve B-1348, Belgium

Jon Grumer and Paul S. Barklem
Theoretical Astrophysics, Department of Physics and Astronomy, Uppsala University, Uppsala SE-75237, Sweden

Shaun G. Ard, Nicholas S. Shuman, and Albert A. Viggiano
Air Force Research Laboratory, Space Vehicles Directorate, Kirtland Air Force Base, NM-87117, USA

(Dated: July 1, 2022)

The double ion storage ring DESIREE has been used in combination with position and time-sensitive detectors to study the mutual neutralisation of N^+ with O^- at 40 meV collision energy. Several previously unassigned spectral features observed in a recent single-pass merged-beams experiment at 7 meV collision energy [Phys. Rev. Lett. **121**, 083401 (2018)], were also observed in the present experiment. It was found that neutralisation channels of the first metastable state of the cation ($N^+(^1D)$, $\tau \approx 256$ s) could explain the majority of these features, while the second metastable state ($N^+(^1S)$, $\tau \approx 0.9$ s) was not found to contribute significantly. The branching ratios into the different electronically excited states of N were determined and found to be in good agreement between the two experiments. Theoretical calculations using the multi-channel Landau-Zener model were found to yield good results for a number of channels, but could not describe some observed contributions, possibly due to the presence of other processes not accounted for in the model.

I. INTRODUCTION

In the Earth's upper atmosphere, where particles are constantly exposed to UV radiation and number densities are low, ionic species exist in what can be described as a cold plasma. In this unique chemical environment, the primary ions are oxygen and nitrogen, and charge reducing reactions involving these species determine many atmospheric phenomena [1], such as ultraviolet equatorial night-glow [2], local heating [3], and isotope fractionation [4]. While plasma ionization and electron-ion recombination reactions involving atmospheric species have been studied extensively in the past [5–8], mutual neutralisation (MN), i.e, charge transfer between two oppositely charged ions, has not been equally well-studied. Technical limitations have often restricted experiments to cross section/reactivity measurements in the high collision energy regime, i.e. $E_{\mathrm{c.m.}} > 1$ eV [9–11]. Although such studies are useful for testing theoretical models, they are generally not relevant to the media where these reactions primarily occur, such as in planetary atmospheres, interstellar molecular clouds, and cool stellar atmospheres [12].

The mutual neutralisation of N^+ with O^- has been intriguing for a long time, due to its high reactivity and large number of reaction pathways, and is attributed to be the first system for which ion-beam MN measurements were performed [13]. In the first experiment, dating back to 1968, the ion beams were merged into a straight interaction region using magnetic deflectors, and a neutral beam detector was employed to monitor the products. Since these initial investigations, apparatus for studies into this type of reactions have remained largely the same, though technical improvements in the 80s and 90s have been made in regard to increasing the signal to noise ratio. Peart and co-workers [14], significantly improved this ratio by implementing single particle detectors, which allowed for the use of smaller currents and effectively reduced space-charge interactions. Subsequently, they implemented time-of-flight-based detectors [15], which allowed the discrimination of neutrals formed by MN from those arising from collisions with residual gas, further reducing uncertainties. These improvements allowed for estimates of the cross section as a function of the collision energy over a wide range (>1 to 100 eV). However, it took close to another 25 years before the reaction was successfully studied in the low collision energy regime. This was achieved in a state-of-the-art merged-beams apparatus developed at UCLouvain, in which two time- and position-sensitive detectors were used in coincidence to determine the three-dimensional spatial separation between the products [16].

Since MN reactions involving atomic ions are largely exothermic, they may result in electronic excitation of the formed neutrals, and the excess energy is distributed

* mathias.poline@fysik.su.se
† rdt@fysik.su.se

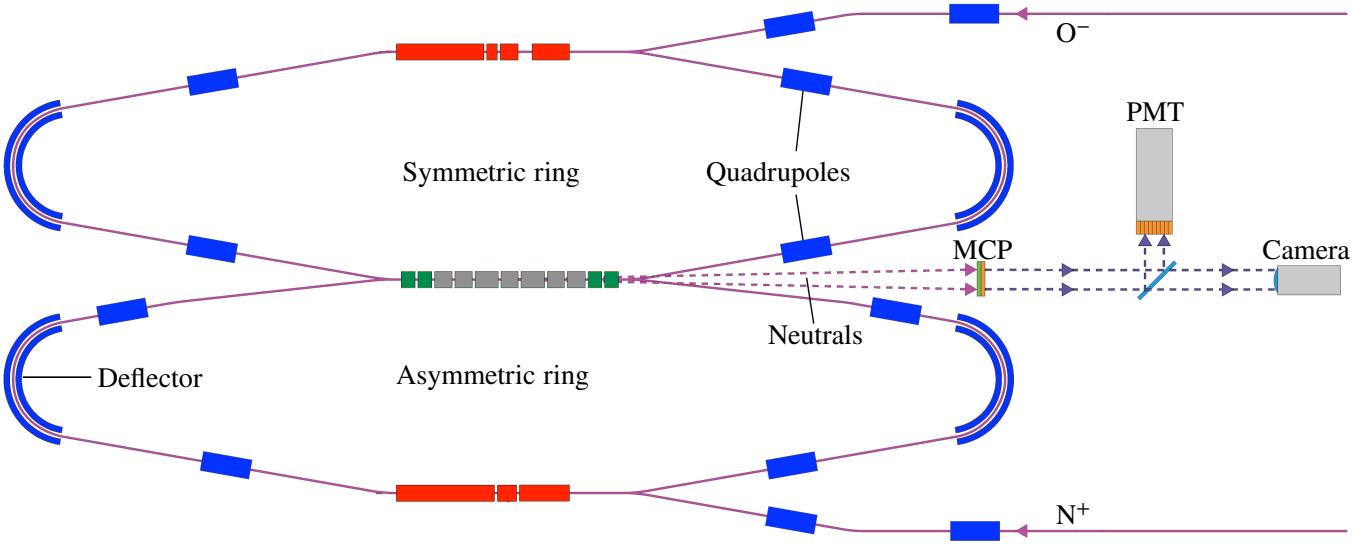

FIG. 1: Schematic of the experimental setup of the double electrostatic storage ion ring DESIREE.

into the two products as kinetic energy. The measured separation between the products can therefore be used to identify the initial and final states of the reaction, and branching ratios can be determined from the distribution of these neutrals on the detector. As MN reaction rates do not solely depend on the exothermicity, but also on several other factors such as long-range interactions between electronic states at their crossing point [17, 18], they are difficult to model accurately. For a complete understanding of the MN process, collision-energy dependent reaction data on the product branching ratios into the open channels is therefore crucial.

In the reaction of N^+ and O^-, the excess energy allows the nitrogen to either capture the electron into the $3p$-subshell (with one of the following LS terms):

$$N^+(^3P) + O^-(^2P) \rightarrow \begin{cases} N(3p\ ^2P^o) + O(^3P) + 0.96\ \text{eV} \\ N(3p\ ^2D^o) + O(^3P) + 1.08\ \text{eV} \\ N(3p\ ^4S^o) + O(^3P) + 1.09\ \text{eV} \\ N(3p\ ^4P^o) + O(^3P) + 1.24\ \text{eV} \\ N(3p\ ^4D^o) + O(^3P) + 1.33\ \text{eV} \\ N(3p\ ^2S^o) + O(^3P) + 1.48\ \text{eV} \end{cases}, \tag{1}$$

or into the $3s$-subshell (with one of these LS terms):

$$N^+(^3P) + O^-(^2P) \rightarrow \begin{cases} N(3s\ ^2P) + O(^3P) + 2.40\ \text{eV} \\ N(3s\ ^4P) + O(^3P) + 2.75\ \text{eV} \end{cases}. \tag{2}$$

Interestingly, de Ruette *et al.* [16] discovered that about 30% of the reactions actually favour a very different pathway, namely:

$$N^+(^3P) + O^-(^2P) \rightarrow N(2s2p^4\ ^4P) + O(^3P) + 2.16\ \text{eV}, \tag{3}$$

i.e, the nitrogen ends up in a core excited configuration. While these experimental results were of high quality, performed with well collimated beams in a high-vacuum environment, the authors also reported the presence of metastable ions in their beams, which gave small but significant contributions in the products-energy spectra. Such effects are often expected in merged beams experiments, and disentangling these contributions from those of pure ground-state reactions can be problematic.

At the double electrostatic storage ring DESIREE [19, 20], these effects can be studied effectively. This modified merged beams apparatus largely resembles previously described experimental techniques, with the important difference being that the ions are not discarded after a single pass but instead are stored and pass through the interaction region many times (see Fig. 1), allowing for radiative de-excitations to take place.

In a recent study [21], the role of metastable ions was investigated in the MN of O^+ with O^-. While short-lived metastable ions were not observed to contribute, long lived metastable ions ($O^+(^2D^o)$, $\tau \approx 3.6$ hours [22]), gave rise to numerous contributions to the product spectra. In the present study, we aim to apply the same treatment to the MN of N^+ and O^-. Information on the metastable contribution is relevant to atmospheric modeling, as photo- and cosmic-ray ionisation processes can result in the formation of metastable ions [23]. Such a study also serves as a stringent test of current theoretical models, since calculations involving metastable ions significantly increase in complexity, due to the increased number of open reaction pathways and the higher electronic angular momenta of the reactants and products.

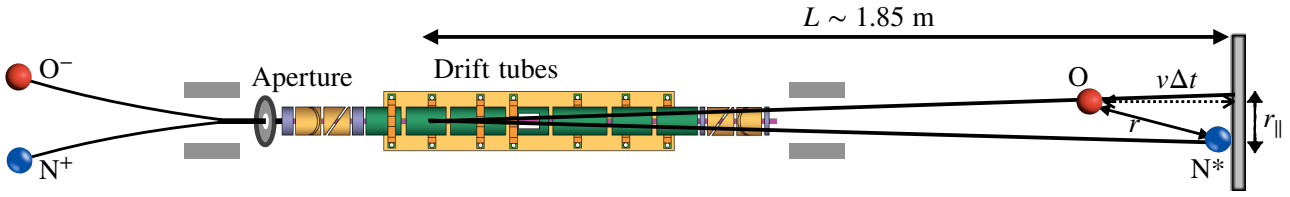

(a)

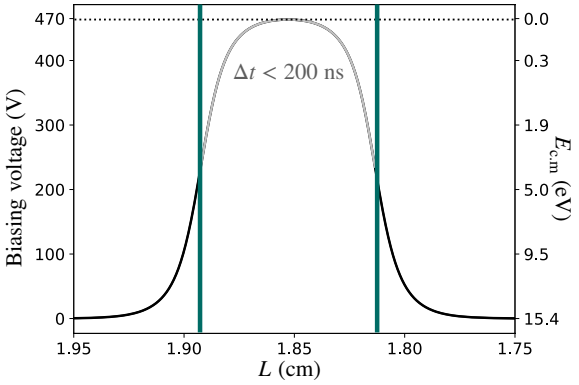

(b)

FIG. 2: (a) Schematic of the merging section and the measured quantities. (b) Simulation of the voltage potential in the biased region. The gray part of the curve represents the portion of the drift tube in which the two ion beams are separated by less than 200 ns in time. The green bars denote the physical size of the drift tube.

II. METHODS

Experimental procedure

For the present experiment, N^+ is produced from an electron cyclotron resonance (ECR) ion source fed with molecular nitrogen as a source gas. The N^+ beam is extracted from the source and accelerated to 7.00 keV. The O^- ions are produced from a TiO cathode using a Source of Negative Ions by Cesium Sputtering (SNICS), and accelerated to 7.00 keV. The quoted beam energies are based on measurements of the actual acceleration voltages on the ion-source platforms. Once the ions of interest are mass selected and injected into the apparatus, the ions retain these velocities, and are stored in rings by the use of deflectors and quadrupole ion-optics. These ion-optical elements are distributed differently among the two rings, in a what can be described as a "symmetric" or "asymmetric" arrangement (see Fig. 1). This design permits the merging of ion beams with different energies into a common straight section, in which charge transfer takes place. In this region, the oppositely charged ions approach one another at relative velocities of about 20 km/s. In order to achieve the lowest collision energy possible, a section of the merged region is biased by a voltage of 470 V. This accelerates and decelerates the cation and anion beams, respectively, such that their relative velocity in the interaction region is close to zero. The resolution of the product kinetic energy release spectra is related to the length of this biased section, which can be controlled through the selection of one to seven drift tubes. The neutral products formed in the reactions are detected by a triple-stack microchannel plate based detector with a phosphor-screen anode [24], from which the resulting fluorescence light is guided by an optical beam splitter to a time-sensitive detector (PMT) and a CMOS-based camera. The event rate is generally low (0.1-1 counts/second), as small ion beam currents are used (typically a few nA), with few false coincidences arising from collisions with residual gas particles or from dark counts in the detectors.

Recently, a set of movable apertures were installed in order to control the beam overlap as well as limit the transverse velocity spread of the interacting ions. These are placed at the entrance and exit of the merged section, as seen in Fig. 2(a), and have diameters ranging from 2.5 to 25 mm. As in previous experiments, pick-up electrodes at the entrance and exit to the merging region measure the beam positions, and two Faraday cups are used to measure the ion currents at the end of the storage cycle. This allows optimisation of the overlap of the two ion beams, as the apertures are controlled, by monitoring ion-beam currents and ion-beam lifetimes. The exit aperture is then removed to allow neutrals to be detected, while the entrance aperture is kept in place, as shown in the figure. This new implementation leads to a significant improvement in the signal to noise ratio, and in a reduction of the transverse velocity spread of the ions with a concomitant decrease in the collision energy, as evidenced in the recent work on the MN of Mg^+ with D^- [25].

Data evaluation

The separation between the two particles, r, as illustrated in Fig. 2(a), is a measure of the kinetic energy release, E_K, through the relationship:

$$r = \left(r_\parallel^2 + (v\Delta t)^2\right)^{1/2} \approx \left(\frac{2(E_K + E_{\mathrm{c.m.}})}{\mu}\right)^{1/2} \frac{L}{v}, \quad (4)$$

where $r_{\parallel}$ is the distance between the products on the imaging detector, Δt their arrival time difference, and v is the average velocity of the ions. The center-of-mass collision energy $E_{\mathrm{c.m.}}$ depends on the applied voltage U in the drift tube region, and the angle between the ions, α, according to:

$$E_{\mathrm{c.m}} = \mu \left[\frac{E_1(U)}{m_1} + \frac{E_2(U)}{m_2} - 2\sqrt{\frac{E_1(U)E_2(U)}{m_1 m_2}}\cos\alpha \right], \tag{5}$$

where E_1 and E_2 are the beam energies, and m_1 and m_2 the masses of the cation and anion, respectively (in this case N^+ and O^-).

In order to achieve the best resolution, a single drift tube was biased in the present experiment. However, as illustrated in Fig. 2(b), this results in large fringe field effects, i.e, the collision energy is high over a significant fraction of the interaction region. MN events occurring at these points will therefore have larger separations r, and this makes it difficult to resolve individual channels. In order to limit this effect, two processes are performed during the data analysis. The first is the exclusion of events with arrival time differences larger than 200 ns. This confines the range of allowed collision energies, as illustrated by the gray line in Fig. 2(b), while still permitting detection of all product channels. The second process makes use of the anisotropy associated with high energy collisions: As the collision energy increases, the products' final velocity vectors are more likely to be along the beam axis, i.e the $v\Delta t$ term tends to dominate in the measured r values. Removing events for which this is the case thus allows to further account for these fringe field effects.

In order to extract the product branching ratios, simulations of the r distributions based on these constrains are performed for each output channel (equation 1-3), and these are then fitted to the experimental data. These are then corrected for the kinetic energy release dependent angular acceptance of the detectors (for more details, see reference [21]).

Theoretical calculations

Theoretical calculations of the partial cross sections for electron transfer into the various final states are performed following the method outlined in Poline *et al.* [21], which largely follows the method described by Zhou & Dickinson [26]. The method employs the multi-channel Landau-Zener model expressed in term of partial waves, and uses an anion centered asymptotic method to determine the coupling matrix elements [27]. The polarisability of N^+ is adopted as $\alpha_1 = 3.67$ a.u. from Éhn and Černušák [28], while for O^-, $\alpha_2 = 21.59$ a.u. is adopted [29].

The $N^+ + O^-$ system is special as one of the channels was found to result in the core-excited configuration state $N(2s2p^4\ {}^4P)$ (equation 3). This would normally require a two-electron process during an MN reaction, i.e the transferred electron would additionally result in excitation of a $2s$ electron to the $2p$ orbital. This was surprising in view of previous theoretical calculations by Zhou & Dickinson [26], which predicted a fairly small cross section for this particular transition due to the nature of the process. However, de Ruette *et al.* [16] showed that, due to configuration interaction, this ^4P state contains contributions from several configurations, which means that the electron transfer can be described as a one-electron process. Taking this into account in the calculations yielded results in better agreement with the experimental observations [16]. It is therefore necessary in the present study to compute the configuration mixing between the atomic states in order to accurately determine the coupling elements. This is especially true for calculations involving metastable ions since most low-lying states of interest of neutral nitrogen are dominated by configurations consisting of the ground state ionic core with an outer electron. Hence if this effect was to be ignored, neutralisation of the first metastable state, $N^+(^1D)$, would be limited to the following channels:

$$N^+(^1D)+O^-(^2P) \rightarrow \begin{cases} N((^1D)\ 3p\ ^2P^o) + O(^3P) + 1.05\ \mathrm{eV} \\ N((^1D)\ 3p\ ^2D^o) + O(^3P) + 1.27\ \mathrm{eV} \\ N((^1D)\ 3s\ ^2D) + O(^3P) + 2.61\ \mathrm{eV} \end{cases}. \tag{6}$$

Recent investigation of the role of the long-lived metastable cation $O^+(^2D^o)$ in the MN of oxygen ions [21] revealed that a number of $O((^4S^o)\ np/nd)$ Rydberg channels also had non-negligible contributions to the spectra, which suggested the presence of core mixing of the $^2D^o$ metastable term in these states. In nitrogen, the metastable state $N^+(^1D)$ lies about 1.9 eV above the ground state, and has a calculated radiative lifetime of 256 seconds [30], which exceeds the storage time used here, and thus its contributions must also be evaluated theoretically to compare with experiment.

To achieve this, an appropriate set of initial $N^+ + O^-$, and final N + O channels are included in the model. Mixing between the different core terms and configurations of N is estimated through multiconfigurational Hartree-Fock (MCHF) calculations using the ATSP2k code [31, 32]. Since the aim of these atomic structure calculations is to provide rough estimates of the mixing effects between different LS-coupled states in the scattering calculations, we keep the number of basis states as small as possible, and also omit relativistic interactions between fine-structure states of the different terms. For the range of possible $2s^2\,2p^2\,nl$ configurations, the correlation models are restricted to the interaction within the configuration itself to facilitate a simple estimate of the mixing between states with different $2p^2$ core terms. Each configuration is treated individually with orbitals optimized in separate MCHF calculations targeting the lowest term only. The obtained orbital wavefunctions

are then used in subsequent configuration interaction calculations including all terms of the configuration under consideration to obtain all its LS eigenstates.

For $2s\,2p^4\,{}^4$P and $2s^2 2p^3\,{}^4$S, ^{2}P, ^{2}D the main mixing occurs between basis states belonging to different configurations. For these cases, correlation is therefore included within the $n \leq 3$ set of configurations constructed through single and double substitutions from either of the four considered reference states, within the orbital set $\{1s,\ 2s,\ 2p,\ 3s,\ 3p,\ 3d\}$. The core $1s^2$ shell is always kept closed. Each of these four terms is optimized in separate MCHF calculations.

III. RESULTS AND DISCUSSION

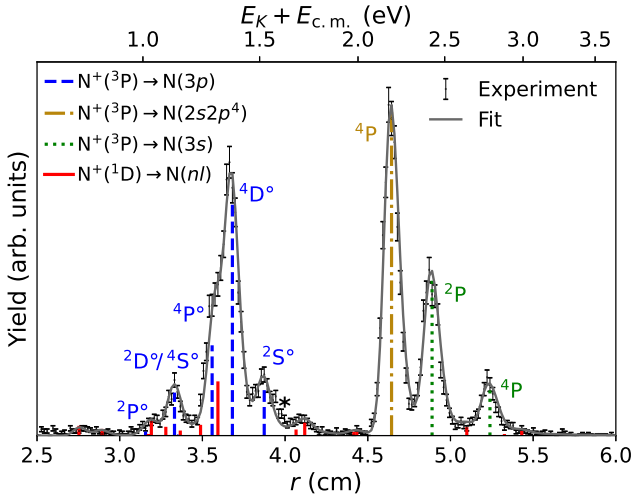

FIG. 3: Yield of neutral N/O pairs as a function of the separation r between the products, at collision energy of 40±10 meV. The full curve results from a fit of simulated distributions, the peak positions for which are shown as bars.

The observed products-energy spectrum measured at $E_{\rm c.m} = 40\pm10$ meV is shown in Fig. 3 as error bars. Note that the quoted collision energy was determined based on the shift of the distributions according to equation 4. The bottom scale of the figure shows the measured separation between the N and O fragments while the top scale shows the corresponding kinetic energy. As can be seen, a multitude of channels are observed, corresponding to equations 1-3. However, smaller features at, for example, 1.0 eV ($\sim$ 3.2 cm) and 1.7 eV ($\sim$ 4.1 cm), do not belong to any of these channels, and instead are found to correspond to channels from the first metastable state of the cation, namely $N^+(^1D)$ ($\tau \approx 256$ s [30]). To highlight this, a fit was performed, including all possible single-electron output channels from the ground and metastable state, and is shown in the figure as a full gray line, with the individual contributions marked as coloured bars at the corresponding $r(E_k)$-values for these channels. Several metastable channels (here shown as red full bars) are then also found at 2.6 eV and 3 eV, with an even larger contribution in the vicinity of the main peaks around 1.3 eV (3.6 cm), which could have substantial effects on the measured branching ratios if neglected. We therefore undertake a re-analysis of the spectrum of de Ruette *et al.* [16], measured at 7 meV collision energy. A new fit, including these metastable contributions, is presented in Fig. 4, with a complete identification of all channels that were found to contribute.

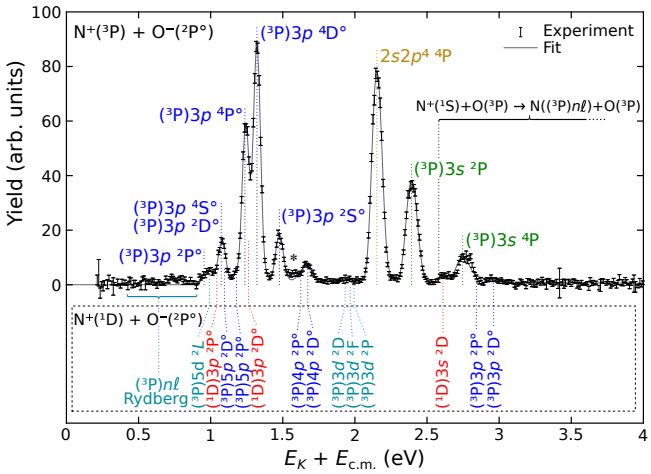

FIG. 4: Yield of neutral N/O pairs as function of the kinetic energy release, at collision energy $E_{\rm c.m.} = 7$ meV. Spectrum is from the single-pass experiment performed by de Ruette *et al.* [16]. Predicted channel positions are shown as dotted lines, with the metastable state's contributions detailed in the bottom panel. The full curve results from a fit of simulated distributions.

The observed additional features are found to be present at the same peak positions as in the present experiment at DESIREE. Hence, we conclude that these previously unassigned contributions arise from the $N^+(^1D)$ metastable state neutralising to a variety of electronic states (see bottom panel of Fig. 4). Here we notice, however, a small mismatch of the fit in the spectra at around 2.7 eV. At these energies, the second metastable state $N^+(^1S)$ ($\tau \approx 0.9$ s) may contribute to the signal, as marked by a vertical line in the spectrum. In contrast, our data at 40 meV collision energy correspond to 10 seconds storage time, which implies that this metastable state would not contribute significantly to the spectra if initially present.

We also observe an excess signal over the fit at around 1.6 eV, here marked with an asterisk. Interestingly, a similar observation is made in the DESIREE experimental spectra (3.9 cm in Fig. 3). The position of this feature is found to correspond to a channel of the ground state cation resulting in $N(2s2p^4\ {}^2D^o) + O(3s\ {}^5S^o)$, i.e a process in which both atoms end up electronically excited. As such processes are believed to be rare, and are difficult to treat theoretically, these were neglected in the

TABLE I: Branching ratios of the MN reaction $N^+(^3P/^1D) + O^-(^2P) \rightarrow N(nl\ ^{2S+1}L) + O(^3P)$. Note that the N($3p$ ^{4}P°) ground state channel (row 4) branching ratio might be overestimated due to the possible presence of the N(3p ^{2}F°) (row 16) metastable state channel at the same energy.

	Mix. coef.[a]	E_K (eV)	Exp 7 meV[b] (%)	Exp 40 meV[c] (%)	Theory[d] (%)
$N^+(^3P) \rightarrow$					
N($3p$ ^{2}P°)	0.99	0.96	0.67±0.13	0.2±0.2	0.49
N($3p$ ^{2}D°, ^{4}S°)	0.99	1.08	2.42±0.15	3.4±1.2	3.27
N($3p$ ^{4}P°)	1.00	1.24	12.44±0.28	10.8±0.8	9.82
N($3p$ ^{4}D°)	1.00	1.33	23.62±0.30	23.8±0.4	28.0
N($3p$ ^{2}S°)	1.00	1.48	5.04±0.17	5.1±0.5	7.38
N($2s2p^4$ ^{4}P)	0.35	2.16	33.38± 0.30	34.3±0.6	33.4
N($3s$ ^{2}P)	1.00	2.40	17.54±0.26	17.1±0.5	15.6
N($3s$ ^{4}P)	1.00	2.75	4.89±0.23	5.3±0.6	0.17
$N^+(^1D) \rightarrow$					
N($n > 5$)	-	<0.98	15.87±1.58	12.3±3.0	-
N($5d$ ^{2}P,D,F)	<0.01	∼0.98	5.90±0.76	9.5±3.1	10^{-6}
N((^{1}D) $3p$ ^{2}P°)	0.99	1.05	4.89±0.92	4.0±2.9	6.8
N($5p$ ^{2}D°)	0.01	1.10	8.90±0.87	3.1±2.3	10^{-3}
N($5p$ ^{2}P°)	0.01	1.18	6.15±1.25	8.2±3.9	10^{-3}
N((^{1}D) $3p$ ^{2}F°)	1.00	1.24	-	-	53.6
N((^{1}D) $3p$ ^{2}D°)	0.99	1.27	25.97±1.81	35.3±10.4	38.8
N($4d$ ^{2}P,D,F)	<0.01	∼1.29	-	-	10^{-4}
N($4p$ ^{2}P°)	0.03	1.63	5.12±0.94	4.1±1.9	0.16
N($4p$ ^{2}D°)	0.03	1.68	11.11±0.90	10.8± 2.1	0.35
N($3d$ ^{2}P,D,F)	<0.01	∼1.9	3.03±0.89	4.2±3.0	0.02
N((^{1}D) $3s$ ^{2}D)	1.00	2.61	5.18±1.55	4.9±2.5	0.21
N($3p$ ^{2}P°)	0.11	2.85	5.50±5.50	-	10^{-3}
N($3p$ ^{2}D°)	0.12	2.97	2.40±2.40	3.6±1.1	0.01

[a] Mixing coefficient of the parental ion's core. [b] Revised results of de Ruette *et al.* [16] [c] Present results [d] Present calculations

fit. We therefore chose here to only present the branching ratios for channels which could be described as single electron processes in our model. These are shown in Table 1, for both the ground state and metastable state of the nitrogen cation, in comparison with our theoretical results.

For the reaction involving the ground state cation, the two experiments (column 5 and 6) are found to mutually agree within the statistical uncertainties and fairly good agreement is observed between experiment and theory. To highlight this, these branching ratios are also shown in Fig. 5 as a function of collision energy.

As can be seen, no change is expected below 1 eV collision energy from the theory, and this is confirmed by the present experimental results. The values differ slightly between theory and experiment but there is agreement concerning the dominating channels. The largest discrepancy is observed for the N($3s$ ^{4}P) channel (lowest full line), for which calculations predict a negligible population. A similar inconsistency was observed in the MN of O^+ with O^- [21] for one of the channels, and is attributed to the theoretical model's low accuracy for the treatment of more energetic transitions, which typically occur at short internuclear distances.

For the reaction involving the metastable cation, the uncertainties of the fit are larger, due to overlap of the peaks with each other as well as with the main channels. Nevertheless, most of the contributions are found to be in agreement between the two experiments, with the N($3p$ ^{2}D°) channel at 1.27 eV found to dominate. On the other hand, theoretical calculations predict that the most prevalent channel is the N($3p$ ^{2}F°) state at 1.25

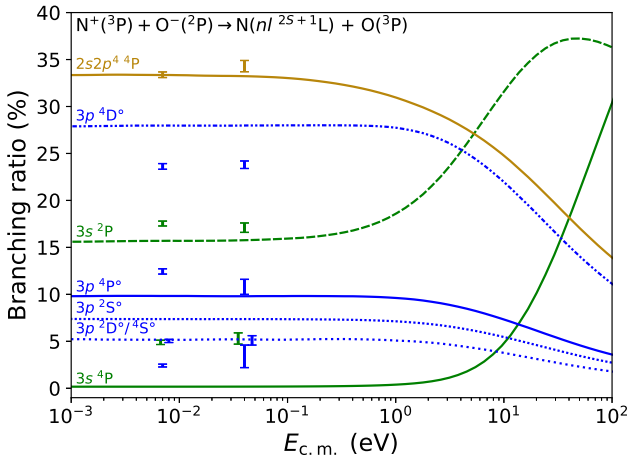

FIG. 5: Branching ratios for the MN reaction of $N^+(^3P)$ with $O^-(^2P)$ as a function of the collision energy. Present theoretical calculations are shown as lines, and experimental results as error bars.

eV. This channnel is not resolved in the two experiments since it coincides largely with the N($3p\ ^4$P^o) ground state channel, and thus was ignored in the fits. As such, the branching ratio for this particular state could be somewhat overestimated.

Noticeably, the theoretical calculations predict that mostly states where the core predominantly corresponds to the metastable $N^+(^1D)$ (see second column) are populated. However, it is clear from the experimental data that states with mainly ^{3}P (ground state) core also contribute to the spectra. For example, at 1.65 eV a clear peak is observed in both spectra, corresponding to neutralisation to the N(^{3}P $4p$) states. While the theoretical calculations predict some mixing of the ^{1}D core to be present in these states (corresponding mixing coefficient $\sim$ 0.03), the computed branching ratios disagree by a large factor. Such discrepancies were also observed in the study of O^+ with O^- [21], and it was believed that these were mainly due to a failure of an approximation used for the calculations of the coupling elements in mixed states. However, the discrepancies in the present study cannot be explained in the same way. The assumption that one-electron processes dominate over multi-electron processes becomes less secure as the mixing coefficient of cores relevant to the one-electron process becomes smaller, since the mixing coefficient determines the scale of the one-electron interaction compared to a possible multi-electron interaction. In the present calculations, the N($2s2p^4\ ^4$P) channel (row 7), is highly mixed (corresponding mixing coefficient of the ground state core is $\sim$0.35), and its branching ratio is predicted in reasonable agreement with experiment, suggesting that here indeed the process is dominated by the one-electron process. In contrast, the channels arising from the metastable state that have small mixing with the $N^+(^1D)$ core, are seen to not agree well with experiment, theory always predicting branching ratios that are significantly smaller. This suggests that there might be a significant multi-electron contribution in these cases.

These results further confirm the limitations of the model for predicting the branching ratios in systems involving excited ions, highlighting the need for development and use of more advanced models. For example, an alternate asymptotic method based on linear combination of atomic orbitals (LCAO) [33–35] has been used to estimate coupling elements, with some success for MN systems with hydrogen as one of the collision partners [25, 36, 37], but cannot, in its present form, capture multi-electron processes. In recent years, *ab initio* methods have been employed to evaluate MN cross sections from quantum chemical calculations of the potentials and couplings [38–40], with some results in excellent agreement with experimental data [41, 42]. However, these have only been applied to simple systems so far, as advanced computational methods are often necessary. Extensions of the present model to include multi-electron processes might therefore be a more suitable approach, but could also turn out to be insufficient to provide an accurate description of the reaction.

IV. CONCLUSIONS

We have studied the mutual neutralisation of N^+ with O^- using a double ion storage ring and theoretical calculations. The branching ratios into the different pairs of electronic states were determined from measurements of the separation and arrival time differences of the neutral pairs at a center-of-mass collision energy of 40 meV. Several spectral features, previously observed in a recent single-pass experiment, were identified to be contributions from the first metastable state of N^+ neutralising to various product states. When taken into account, the results of the two experiments, as well as theory, are found to be in fairly good agreement for the ground state cation, while theoretical calculations fails to predict correctly several observed contributions from the metastable cation, possibly due to the presence of processes not accounted for in the model, such as multi-electron processes.

The present experiment also serves to characterize the present status of DESIREE in terms of the resolution and general quality of the data that can be achieved after a recent upgrade improving the collimation of the ion beams.

CONFLICTS OF INTEREST

There are no conflicts to declare.

ACKNOWLEDGEMENTS

This material is based upon work supported by the Air Force Office of Scientific Research under Award No. FA9550-19-1-7012. This work was performed at the Swedish National Infrastructure, DESIREE (Swedish Research Council Contract No. 2017-00621 and 2021-00155). AD and XU acknowledge support from the Fonds de la Recherche Scientifique–FNRS under grant No. 4.4504.10 and thank the Belgian State for the grant allocated by Royal Decree for research in the domain of controlled thermonuclear fusion. XU is a Senior Research Associate of the Fonds de la Recherche Scientifique-FNRS. JG, HTS and PSB acknowledge funding from the Swedish Research Council (2020-05467, 2018-04092 and 2020-03404).

[1] R. P. Wayne, *Chemistry of atmospheres* (Clarendon Press, Oxford (UK), 1991).

[2] J. Qin, J. J. Makela, F. Kamalabadi, and R. R. Meier, J. Geophys. Res. Space Phys. **120**, 10116 (2015), https://doi.org/10.1002/2015JA021687.

[3] D. Hamlin and B. Myers, Planet. Space Sci. **22**, 1343 (1974), https://doi.org/10.1016/0032-0633(74)90056-7.

[4] J. L. Fox and A. Hać, J. Geophys. Res. Planets **102**, 9191 (1997), https://doi.org/10.1029/97JE00086.

[5] E. Krishnakumar and S. Srivastava, Int. J. Mass Spectrom. Ion Processes **113**, 1 (1992), https://doi.org/10.1016/0168-1176(92)87037-F.

[6] R. Peverall, S. Rosén, J. R. Peterson, M. Larsson, A. Al-Khalili, L. Vikor, J. Semaniak, R. Bobbenkamp, A. Le Padellec, A. N. Maurellis, and W. J. van der Zande, J. Chem. Phys. **114**, 6679 (2001), https://doi.org/10.1063/1.1349079.

[7] L. Vejby-Christensen, D. Kella, H. B. Pedersen, and L. H. Andersen, Phys. Rev. A **57**, 3627 (1998), https://doi.org/10.1103/PhysRevA.57.3627.

[8] J. R. Peterson, A. Le Padellec, H. Danared, G. H. Dunn, M. Larsson, A. Larson, R. Peverall, C. Strömholm, S. Rosén, M. af Ugglas, and W. J. van der Zande, J. Chem. Phys. **108**, 1978 (1998), https://doi.org/10.1063/1.475577.

[9] S. Szucs, M. Karemera, M. Terao, and F. Brouillard, J. Phys. B At. Mol. Opt. **17**, 1613 (1984), https://doi.org/10.1088/0022-3700/17/8/021.

[10] B. Peart and D. A. Hayton, J. Phys. B At. Mol. Opt. **27**, 2551 (1994), https://doi.org/10.1088/0953-4075/27/12/013.

[11] R. Padgett and B. Peart, J. Phys. B At. Mol. Opt. **31**, L995 (1998), https://doi.org/10.1088/0953-4075/31/24/004.

[12] P. S. Barklem, A. K. Belyaev, and M. Asplund, A&A **409**, L1 (2003), https://doi.org/10.1051/0004-6361:20031199.

[13] W. Aberth, J. R. Peterson, D. C. Lorents, and C. J. Cook, Phys. Rev. Lett. **20**, 979 (1968), https://doi.org/10.1103/PhysRevLett.20.979.

[14] B. Peart, S. J. Foster, and K. Dolder, J. Phys. B At. Mol. Opt. **22**, 1035 (1989), https://doi.org/10.1088/0953-4075/22/7/012.

[15] D. A. Hayton and B. Peart, J. Phys. B At. Mol. Opt. **26**, 2879 (1993), https://doi.org/10.1088/0953-4075/26/17/020.

[16] N. de Ruette, A. Dochain, T. Launoy, R. F. Nascimento, M. Kaminska, M. H. Stockett, N. Vaeck, H. T. Schmidt, H. Cederquist, and X. Urbain, Phys. Rev. Lett. **121**, 083401 (2018), https://doi.org/10.1103/PhysRevLett.121.083401.

[17] L. Landau, Phys. Z. Sowjetunion **2**, 118 (1932).

[18] C. Zener and R. H. Fowler, Proc. Math. Phys. Eng. Sci. **137**, 696 (1932), https://doi.org/10.1098/rspa.1932.0165.

[19] R. D. Thomas, H. T. Schmidt, G. Andler, M. Björkhage, M. Blom, L. Brännholm, E. Bäckström, H. Danared, S. Das, N. Haag, P. Halldén, F. Hellberg, A. I. S. Holm, H. A. B. Johansson, A. Källberg, G. Källersjö, M. Larsson, S. Leontein, L. Liljeby, P. Löfgren, B. Malm, S. Mannervik, M. Masuda, D. Misra, A. Orbán, A. Paál, P. Reinhed, K.-G. Rensfelt, S. Rosén, K. Schmidt, F. Seitz, A. Simonsson, J. Weimer, H. Zettergren, and H. Cederquist, Rev. Sci. Instrum. **82**, 065112 (2011), https://doi.org/10.1063/1.3602928.

[20] H. T. Schmidt, R. D. Thomas, M. Gatchell, S. Rosén, P. Reinhed, P. Löfgren, L. Brännholm, M. Blom, M. Björkhage, E. Bäckström, J. D. Alexander, S. Leontein, D. Hanstorp, H. Zettergren, L. Liljeby, A. Källberg, A. Simonsson, F. Hellberg, S. Mannervik, M. Larsson, W. D. Geppert, K. G. Rensfelt, H. Danared, A. Paál, M. Masuda, P. Halldén, G. Andler, M. H. Stockett, T. Chen, G. Källersjö, J. Weimer, K. Hansen, H. Hartman, and H. Cederquist, Rev. Sci. Instrum. **84**, 055115 (2013), https://doi.org/10.1063/1.4807702.

[21] M. Poline, A. Dochain, S. Rosén, J. Grumer, M. Ji, G. Eklund, A. Simonsson, P. Reinhed, M. Blom, N. S. Shuman, S. G. Ard, A. A. Viggiano, M. Larsson, H. Cederquist, H. T. Schmidt, H. Zettergren, X. Urbain, P. S. Barklem, and R. D. Thomas, Phys. Chem. Chem. Phys. **23**, 24607–24616 (2021), https://dx.doi.org/10.1039/D1CP03977F.

[22] E. C. Zipf, Can. J. Chem. **47**, 1863 (1969), https://doi.org/10.1139/v69-305.

[23] M. H. Rees, *Physics and Chemistry of the Upper Atmosphere* (Cambridge University Press, 1989) https://doi.org/10.1017/CBO9780511573118.

[24] S. Rosén, H. T. Schmidt, P. Reinhed, D. Fischer, R. D. Thomas, H. Cederquist, L. Liljeby, L. Bagge, S. Leontein, and M. Blom, Rev. Sci. Instrum. **78**, 113301 (2007), https://doi.org/10.1063/1.2814030.

[25] J. Grumer, G. Eklund, A. M. Amarsi, P. S. Barklem, S. Rosén, M. Ji, A. Simonsson, H. Cederquist, H. Zettergren, and H. T. Schmidt, Phys. Rev. Lett. **128**, 033401 (2022), https://doi.org/10.1103/PhysRevLett.128.033401.

[26] X. Zhou and A. Dickinson, Nucl. Instrum. Methods B **124**, 5 (1997), https://doi.org/10.1016/S0168-583X(96)00922-6.

[27] R. Janev, Adv. At. Mol. Opt. Phys. **12**, 1 (1976), https://doi.org/10.1016/S0065-2199(08)60041-X.

[28] L. Éhn and I. Černušák, Int. J. Quantum Chem. **121**, e26467 (2021), https://doi.org/10.1002/qua.26467.

[29] A. Dalgarno, Adv. Phys. **11**, 281 (1962), https://doi.org/10.1080/00018736200101302.

[30] C. Froese Fischer and G. Tachiev, At. Data Nucl. **87**, 1 (2004), https://doi.org/10.1016/j.adt.2004.02.001.

[31] C. Froese Fischer, G. Tachiev, G. Gaigalas, and M. R. Godefroid, Comput. Phys. Commun. **176**, 559 (2007), https://doi.org/10.1016/j.cpc.2007.01.006.

[32] C. Fischer, T. Brage, and P. Jönsson, *Computational Atomic Structure: An MCHF Approach (1st ed.)* (Routledge, 1997) https://doi.org/10.1201/9781315139982.

[33] R. Grice and D. Herschbach, Mol. Phys. **27**, 159 (1974), https://doi.org/10.1080/00268977400100131.

[34] S. Adelman and D. Herschbach, Mol. Phys. **33**, 793 (1977), https://doi.org/10.1080/00268977700100731.

[35] P. S. Barklem, Phys. Rev. A **93**, 042705 (2016), https://doi.org/10.1103/PhysRevA.93.042705.

[36] G. Eklund, J. Grumer, S. Rosén, M. Ji, N. Punnakayathil, A. Källberg, A. Simonsson, R. D. Thomas, M. H. Stockett, P. Reinhed, P. Löfgren, M. Björkhage,

M. Blom, P. S. Barklem, H. Cederquist, H. Zettergren, and H. T. Schmidt, Phys. Rev. A **102**, 012823 (2020), https://doi.org/10.1103/PhysRevA.102.012823.

[37] G. Eklund, J. Grumer, P. S. Barklem, S. Rosén, M. Ji, A. Simonsson, R. D. Thomas, H. Cederquist, H. Zettergren, and H. T. Schmidt, Phys. Rev. A **103**, 032814 (2021), https://doi.org/10.1103/PhysRevA.103.032814.

[38] A. K. Belyaev, B. Lepetit, and F. X. Gadéa, Phys. Rev. A **90**, 062701 (2014), https://doi.org/10.1103/PhysRevA.90.062701.

[39] S. Nkambule, P. Nurzia, and Å. Larson, Chem. Phys. **462**, 23 (2015), https://doi.org/10.1016/j.chemphys.2015.08.006.

[40] Å. Larson, J. Hörnquist, P. Hedvall, and A. E. Orel, J. Chem. Phys. **151**, 214305 (2019), https://doi.org/10.1063/1.5128357.

[41] H. Croft, A. S. Dickinson, and F. X. Gadéa, J. Phys. B: At. Mol. Opt. Phys. **32**, 81 (1999), https://doi.org/10.1088/0953-4075/32/1/008.

[42] T. Launoy, J. Loreau, A. Dochain, J. Liévin, N. Vaeck, and X. Urbain, ApJ **883**, 85 (2019), https://doi.org/10.3847/1538-4357/ab3346.